



RESEARCH ARTICLE

10.1002/2014GB004809

Key Points:

- Stable isotope ratios of rainwater ammonium were measured at Bermuda
- Rainwater ammonium isotopes do not vary with air mass history
- Isotopes and simple steady state box model suggest ocean ammonia source

Supporting Information:

- Readme
- Figures S1–S5
- Tables S1–S3

Correspondence to:

K. E. Altieri,
kaltieri@princeton.edu

Citation:

Altieri, K. E., M. G. Hastings, A. J. Peters, S. Oleynik, and D. M. Sigman (2014), Isotopic evidence for a marine ammonium source in rainwater at Bermuda, *Global Biogeochem. Cycles*, 28, doi:10.1002/2014GB004809.

Received 15 JAN 2014

Accepted 4 SEP 2014

Accepted article online 17 SEP 2014

Isotopic evidence for a marine ammonium source in rainwater at Bermuda

K. E. Altieri^{1,2}, M. G. Hastings¹, A. J. Peters³, S. Oleynik², and D. M. Sigman²

¹Department of Geological Sciences and Environmental Change Initiative, Brown University, Providence, Rhode Island, USA,

²Department of Geosciences, Princeton University, Princeton, New Jersey, USA, ³Bermuda Institute of Ocean Sciences, St. Georges, Bermuda

Abstract Emissions of anthropogenic nitrogen (N) to the atmosphere have increased tenfold since preindustrial times, resulting in increased N deposition to terrestrial and coastal ecosystems. The sources of N deposition to the ocean, however, are poorly understood. Two years of event-based rainwater samples were collected on the island of Bermuda in the western North Atlantic, which experiences both continent- and ocean-influenced air masses. The rainwater ammonium concentration ranged from 0.36 to 24.6 μM , and the ammonium $\delta^{15}\text{N}$ from -12.5 to 0.7‰ ; and neither has a strong relationship with air mass history ($6.0 \pm 4.2 \mu\text{M}$, $-4.1 \pm 2.6\text{‰}$ in marine air masses and $5.9 \pm 3.2 \mu\text{M}$, $-5.8 \pm 2.5\text{‰}$ in continental air masses; numerical average \pm standard deviation). A simple box model suggests that the ocean can account for the concentration and isotopic composition of ammonium in marine rainwater, consistent with the lack of correlation between ammonium $\delta^{15}\text{N}$ and air mass history. If so, ammonium deposition reflects the cycling of N between the ocean and the atmosphere, rather than representing a net input to the ocean. The $\delta^{15}\text{N}$ data appear to require that most of the ammonium/a flux to the ocean is by dissolution in surface waters rather than atmospheric deposition. This suggests that the atmosphere and surface ocean are near equilibrium with respect to air/sea gas exchange, implying that anthropogenic ammonia will equilibrate near the coast and not reach the open marine atmosphere. Whereas $\sim 90\%$ of the ammonium deposition to the global ocean has previously been attributed to anthropogenic sources, the evidence at Bermuda suggests that the anthropogenic contribution could be much smaller.

1. Introduction

The emission of anthropogenic nitrogen (N) to the atmosphere and its subsequent deposition has increased tenfold since preindustrial times [Galloway *et al.*, 2004]. The impacts of increased N deposition to terrestrial and coastal systems are well studied [e.g., Elser *et al.*, 2009; Paerl *et al.*, 2002]; however, the implications for open ocean N biogeochemistry remain uncertain [Duce *et al.*, 2008]. Both anthropogenic and natural processes impact the amount and form of N deposited in remote marine environments. Although clear increases in nitrate deposition have been detected as a result of increased anthropogenic emissions of N oxides ($\text{NO} + \text{NO}_2 = \text{NO}_x$) [Elliott *et al.*, 2007; Galloway *et al.*, 2003; Hastings *et al.*, 2009], large uncertainties in both regional and global budgets of ammonia/um ($\text{NH}_x = \text{NH}_3 + \text{NH}_4^+$) emissions and deposition remain [Clarisse *et al.* [2009], and references therein], especially with regard to the sign and magnitude of the NH_3 air-sea flux [Johnson *et al.*, 2008; Quinn *et al.*, 1996].

Identifying the sources of N deposition to the open ocean is critical for understanding the biogeochemical impacts of human activities. If the N deposition is terrestrial in origin, it represents an external input to the open ocean, and that input is influenced heavily by anthropogenic activities and can be expected to rise into the future [Duce *et al.*, 2008]. In contrast, if the N originates from the ocean and cycles through the atmosphere before being redeposited, it is not a net input of N to the ocean. Inorganic N is the dominant form of N deposition in both polluted [Cornell *et al.*, 2003; Russell *et al.*, 1998] and remote sites [Duce *et al.*, 2008; Galloway *et al.*, 1996, 1982, 1989]. The N and oxygen (O) isotopes of nitrate have been used to identify sources of NO_x contributing to nitrate deposition in both polluted [Elliott *et al.*, 2007; Freyer, 1978; Wankel *et al.*, 2010] and remote [Altieri *et al.*, 2013; Hastings *et al.*, 2003; Morin *et al.*, 2009] locations. While the N isotopes of ammonium (NH_4^+) in wet deposition have been used less frequently as a source tracer, there is evidence that continental and marine aerosol ammonium have different ranges in $^{15}\text{N}/^{14}\text{N}$ [Jickells *et al.*, 2003]. The relationship between the N isotopes of NH_4^+ and nitrate might also shed light on potential

interconversions of inorganic N as it is transported from polluted coastal regions to the open ocean. With these goals in mind, we undertook the first study of the isotopic composition of NH_4^+ in rainwater on an event basis in the marine atmosphere.

1.1. Ammonium in the Marine Atmosphere

Global NH_3 emissions are dominated by human activities including agriculture, animal husbandry, and biomass burning, while natural emissions are much smaller and include vegetation and oceanic emissions [Erisman *et al.*, 2007]. However, there are great uncertainties in the rates of NH_3 emission for all sources and at all scales [Galloway *et al.*, 2008]. Due to the high deposition velocity of NH_3 and its rapid conversion to particulate ammonium ($\text{NH}_4^+_{(p)}$), NH_3 is rarely transported more than 10–100 km from its source [Asman *et al.*, 1998]. The turnover time of NH_3 is estimated to be 0.5 to 1.8 days, such that air masses over the open ocean are expected to contain mostly ocean-derived NH_3 [Quinn *et al.*, 1987]. Wet deposition is the ultimate removal mechanism for NH_x ($\text{NH}_3 + \text{NH}_4^+$).

Ammonia is the dominant base in the troposphere and neutralizes the acidic gases produced by the oxidation of SO_2 and NO_x . Ammonia partitions rapidly between the gas phase and highly acidic submicron aerosol phase by neutralization reactions with sulfuric and nitric acids, forming fine mode ammonium nitrate (NH_4NO_3), ammonium sulfate ($(\text{NH}_4)_2\text{SO}_4$), and ammonium bisulfate (NH_4HSO_4) [Clegg *et al.*, 1998]. Ammonium undergoes chemical and physical processing as polluted continental air masses are transported into the marine atmosphere. Concentrations of both NH_3 and HNO_3 decrease due to dilution with relatively clean marine air, causing fine mode NH_4NO_3 aerosols to dissociate; thus, it is likely that any $\text{NH}_4^+_{(p)}$ exported off the coast of North America would be as fine mode ammonium sulfate aerosols [Allen *et al.*, 1989] rather than NH_4NO_3 .

According to Galloway *et al.* [2008], the net flux of NH_3 was from the ocean to land during preindustrial times and has likely reversed due to anthropogenic activities. A recent study in which both oceanic and atmospheric NH_3 concentrations were measured found the flux of NH_3 to be out of the ocean at low latitudes and into the ocean at high latitudes, with the direction of the flux primarily driven by temperature [Johnson *et al.*, 2008]. There is no way to discern the anthropogenic impact on atmospheric or oceanic NH_3 concentration measurements, rendering it a challenge to identify how the flux has been impacted by human activities. It is assumed that NH_3 is not in Henry's law equilibrium across the air/sea interface as the lifetime of NH_3 removal to particles is much faster than the exchange equilibration time, although this is still an open question [Norman and Leck, 2005; Quinn *et al.*, 1992]. In a marine environment, the lifetime of NH_3 gas with respect to particle formation is thought to be very low, ~ 30 min [Quinn *et al.*, 1992]. However, this is critically dependent on the NH_4^+ to non-sea salt sulfate (nss-SO_4^{2-}) ratio as there must be excess acidic aerosol present for the reaction to proceed this quickly.

1.2. Previous N Isotope Work

Previous studies have used the N and O isotopes of nitrate (NO_3^-) as a tool for distinguishing nitrate sources and chemical formation pathways in polluted [Elliott *et al.*, 2007; Freyer, 1978] and open ocean environments [Altieri *et al.*, 2013; Hastings *et al.*, 2003; Morin *et al.*, 2009]. Based on a year of rainwater samples, Hastings *et al.* [2003] showed that NO_3^- in Bermuda rain has higher $\delta^{15}\text{N-NO}_3^-$ and lower $\delta^{18}\text{O-NO}_3^-$ in the warm season (April to September; -2.1‰ and 68.6‰) as compared to the cool season (October to March; -5.9‰ and 76.9‰). During the warm season, it appears that there is substantial NO_3^- in Bermuda rain that has an isotopic signature distinct from the NO_3^- coming off North America, implying an alternative NO_3^- source over the North Atlantic.

The same Bermuda rainwater samples analyzed for NO_3^- -N and -O isotopes [Hastings *et al.*, 2003] were analyzed for total dissolved N, allowing for calculation of the $\delta^{15}\text{N}$ of "reduced N" ($\text{RN} = \text{NH}_4^+ + \text{water soluble organic N (WSON)}$) [Knapp *et al.*, 2010]. Total reduced N shows no statistically significant seasonal variation in concentration or flux. However, similar to nitrate, the reduced N does show significant seasonal variability in mass-weighted average $\delta^{15}\text{N}$ (-2.7‰ in the cool season and 1.5‰ in the warm season). Knapp *et al.* [2010] did not differentiate NH_4^+ isotopic values from the WSON isotopic values; thus, it is not known which species are controlling the isotopic signals or the seasonality observed in $\delta^{15}\text{N-RN}$.

There are relatively few studies of atmospheric $\delta^{15}\text{N-NH}_4^+$ in aerosols in the marine environment; and to our knowledge, no studies of rainwater $\delta^{15}\text{N-NH}_4^+$ in the marine environment. In a coastal United States site significantly influenced by continental emissions, $\delta^{15}\text{N-NH}_4^+$ in rainwater ranged from -8 to 8‰ , with a median value of -0.5‰ [Russell *et al.*, 1998]. They found a spring peak in NH_4^+ concentration with a corresponding minimum in $\delta^{15}\text{N-NH}_4^+$, which they attribute to greater agricultural emissions of NH_3 depleted in ^{15}N due to kinetic isotope fractionation during volatilization.

To investigate the sources of atmospheric inorganic N deposition to the ocean and the cycling of N between the lower atmosphere and surface ocean, 2 years of event-based rainwater samples were collected on the island of Bermuda. Samples were analyzed for major ion concentrations and N isotope ratios of NH_4^+ ; NOAA Hybrid Single-Particle Lagrangian Integrated Trajectory (HYSPPLIT) was used to determine air mass history for each rainwater sample, which was used to classify events as originating over North America (continental) or as marine in origin. To test the hypothesis that ocean emissions of NH_3 could represent the dominant source of NH_4^+ measured in marine rainwater, a simple steady state box model was developed for the concentrations and isotopic compositions of aqueous ammonia/ammonium in subtropical surface waters ($\text{NH}_3(\text{sw})$ and $\text{NH}_4^+(\text{sw})$) and ammonia gas and ammonium particles ($\text{NH}_3(\text{g})$ and $\text{NH}_4^+(\text{p})$) in the overlying atmosphere.

2. Methods

2.1. Sample Collection

Rainwater samples were collected on the island of Bermuda (32.27°N , 64.87°W) from 1 July 2009 to 16 September 2011 ($n = 98$) at an active ambient air quality monitoring site (station Prospect). Ambient air quality at this location is characterized by low levels of NO_x , SO_2 , and particulate matter (particulate matter $10\ \mu\text{m}$ (PM_{10}), and $\text{PM}_{2.5}$) (A. Peters, unpublished data, 2013). The site is located atop a water catchment 65 m above sea level. It is unobstructed in all directions and is the second highest point on the island. Rainwater samples were collected in acid washed polyethylene buckets using an automatic rain collector (Aerochem Metrics model 301). Samples were collected on an event basis, retrieved daily, and then frozen to limit microbial degradation of organic matter and consumption of inorganic nutrients. For all samples, the pH, rain volume, and conductivity are measured before being stored at -20°C . Field blanks were collected by placing 200 mL of deionized water into the rainwater collector overnight and then collecting the water in the same way as a rainwater sample. The full suite of chemical analyses was also performed on the field blanks to assess possible contamination from the collector and/or sample handling.

An additional 11 rainwater samples were collected on an event basis at the Bermuda Institute of Ocean Sciences from 2 July 2010 to 13 August 2010, and four rainwater samples were collected at the Tudor Hill Marine-Atmospheric Sampling Observatory tower located 23 m above sea level in March of 2010. These samples are treated in the same manner as those collected at station Prospect.

2.2. Anion and Cation Concentrations

The rainwater samples were analyzed by ion chromatography for anions (Cl^- , NO_3^- , and SO_4^{2-}) and cations (Na^+ , K^+ , Ca^{2+} , Mg^{2+} , and NH_4^+) using an ICS-1600 and ICS-1500, respectively (Thermo Scientific Dionex, Sunnyvale, USA). Anions were analyzed using an IonPac AS14A 5 μm analytical column ($3 \times 150\ \text{mm}$) with an IonPac AG14A 5 μm guard column ($3 \times 30\ \text{mm}$). The mobile phase was a solution of 8 mM Na_2CO_3 and 1 mM NaHCO_3 . Cations were separated and quantified using an IonPac CS16 analytical column ($5 \times 250\ \text{mm}$) with an IonPac CG16 guard column ($5 \times 50\ \text{mm}$). Methanesulfonic acid (47 mM) was used as the eluent. Calibration curves for each analyte were generated using 5 points over the range of 1 to 1000 μM . The instrument detection limits (defined as the concentration calculated to produce a peak height 3 times that of a blank) were 0.29 μM for NH_4^+ , 0.17 μM for NO_3^- , 0.11 μM for Na^+ , 0.08 μM for SO_4^{2-} , 0.04 μM for Cl^- , 0.23 μM for K^+ , 0.40 μM for Mg^{2+} , and 0.17 μM for Ca^{2+} . Ammonium concentrations were also measured on a subset of samples using the orthophthaldialdehyde fluorometric method [Holmes *et al.*, 1998]. Typical sample reproducibility was $\pm 0.4\ \mu\text{M}$ (± 1 standard deviation). Non-sea salt sulfate concentrations are calculated using equation (1), with species in $\mu\text{eq L}^{-1}$ [Keene *et al.*, 1986]:

$$\text{nss} - \text{SO}_4^{2-} = [\text{SO}_4^{2-}] - 0.1555 \times [\text{Na}^+] \quad (1)$$

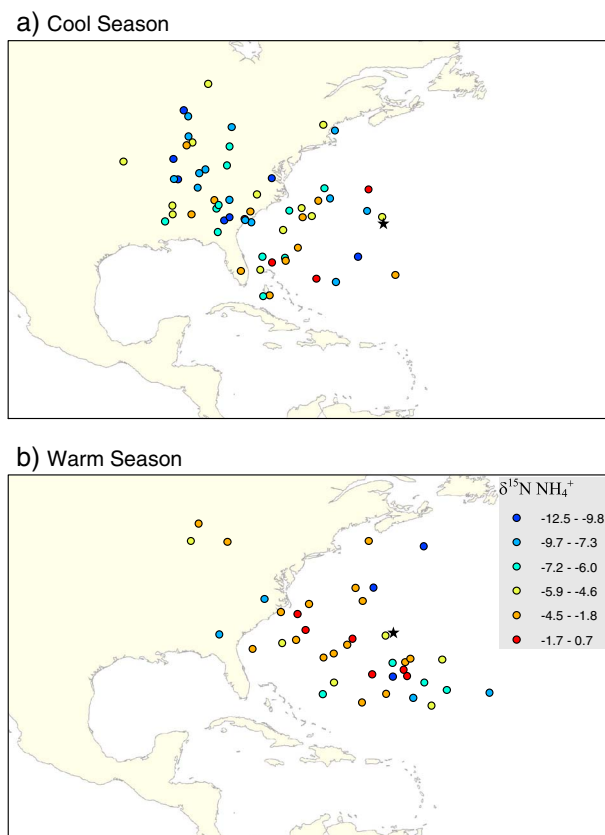


Figure 1. Geographic distribution of samples at 36 h before reaching Bermuda (shown as star) based on NOAA HYSPLIT model back trajectories. Colored symbols represent $\delta^{15}\text{N-NH}_4^+$ for (a) the cool season samples and (b) the warm season samples.

product N_2O is 25 nmol N, as one N atom in the product N_2O is from the azide buffer reagent and one is from the sample NO_2^- . The full reaction blank associated with the conversion from NH_4^+ to N_2O is typically 2–3 nmol N. All samples were run in duplicate at least, with greater than 60% of the samples analyzed in triplicate or more. The pooled standard deviation for all measurements of IAEA-N1 and IAEA-N2 ($n = 53$ and $n = 54$, respectively) is 0.81 and 0.63‰, respectively (Table S1 in the supporting information). The pooled standard deviation from all replicate analyses of samples is 1.2‰.

2.4. HYSPLIT Air Mass Back Trajectory Analysis

To determine the source regions for each rainwater event, air mass back trajectories were computed for all sample days using NOAA's Hybrid Single-Particle Lagrangian Integrated Trajectory model (HYSPLIT v 4) with National Centers for Environmental Prediction Global Data Assimilation System output. HYSPLIT is used to compute the trajectory of a suspended particle backward in time (36–72 h) from a specified point, the island of Bermuda in this case, using a simple particle dispersion simulation and meteorological data. It is accessed via the NOAA ARL READY website at <http://www.arl.noaa.gov/ready/hysplit4.html> (NOAA Air Resources Laboratory, Silver Spring, Maryland). Three-dimensional trajectories were determined at three altitudes: 100 m, 2000 m, and 5000 m. Sensitivity tests to changes in initial conditions indicated that the main sources of uncertainty in the final trajectory were the starting time and the altitude, hence the use of multiple altitudes for each back trajectory. To deal with the variability associated with starting time, trajectories were run starting every hour during the rain event, or if there was uncertainty in the timing of the rain event, trajectories were run starting every hour that the sample bucket was deployed (i.e., all 24 h). The duration of the rain event was determined by cross-referencing sample collection dates with the meteorological observation archive on the Bermuda National Weather Service website (www.weather.bm). Five mean trajectories were extracted from the multiple trajectories

2.3. Ammonium Isotopic Analysis

Measurements of the $^{15}\text{N}/^{14}\text{N}$ of NH_4^+ were made by quantitatively oxidizing NH_4^+ to nitrite (NO_2^-) using hypobromite [Zhang *et al.*, 2007] followed by the reduction of NO_2^- to N_2O using a 1:1 sodium azide and acetic acid buffer solution [McIlvin and Altabet, 2005]. All samples with NH_4^+ concentration greater than $5 \mu\text{M}$ were diluted with ultrapure Milli-Q water to $5 \mu\text{M}$, and 2.5 mL of sample was aliquoted into a combusted glass vial for a final $[\text{NH}_4^+-\text{N}]$ of 12.5 nmol. All reagents were scaled accordingly.

The ion current ratios (m/z 45/44 and 46/44) of the resultant N_2O were measured using a modified GasBench II in line to a Thermo DeltaVPlus isotope ratio mass spectrometry [Sigman *et al.*, 2001], allowing the determination of the $^{15}\text{N}/^{14}\text{N}$. Individual analyses are referenced to injections of N_2O from a pure gas cylinder and then standardized through comparison to replicates of two internationally recognized reference materials: International Atomic Energy Agency (IAEA)-N1 ($\delta^{15}\text{N} = 0.43\text{‰}$ versus N_2 in air) and IAEA-N2 ($\delta^{15}\text{N} = 20.32\text{‰}$ versus N_2 in air) [Bohlke *et al.*, 1993]. When starting with 12.5 nmol of sample N, the

Table 1. The Average ± 1 SD (n) Concentrations and Isotopic Ratios of N in Rainwater Ammonium Binned by the Source Region of the Event Air Mass Back Trajectory (AMBT)^a

	Marine AMBT	Continental AMBT	Coastal AMBT	Average of All Data
^b [NH ₄ ⁺] (μM)	6.03 ± 4.15 (57)	5.92 ± 3.23 (37)	7.79 ± 2.96 (4)	6.02 ± 3.74 (98)
^c δ ¹⁵ N NH ₄ ⁺ (‰)	^e −4.1 ± 2.6	^e −5.8 ± 2.5	−5.8 ± 2.3	−4.9 ± 2.7
^d δ ¹⁵ N NH ₄ ⁺ (‰)	^e −4.9 ± 3.0	^e −6.4 ± 2.6	−5.4 ± 2.4	−5.5 ± 2.9

^aThe number of samples measured for ammonium concentrations and isotopes in each category is in parentheses. Note that the ammonium concentrations are for samples measured for isotopes and thus do not include samples with [NH₄⁺] < 2.0 μM. The volume-weighted average of all data, including those samples, is 4.08 μM.

^bVolume-weighted average.

^cMass-weighted average.

^dNumerical average.

^eStatistically different means at 95% confidence interval, independent *t* test assuming unequal variance, $p < 0.05$.

associated with a single rain event through HYSPLIT's clustering algorithm, which calculates the mean trajectory by averaging overall of the input trajectories at every hour (example trajectories in Figures S1 and S2).

3. Results

3.1. HYSPLIT Air Mass Back Trajectory

The computed and clustered back trajectories from the NOAA HYSPLIT model for the duration of each rain event show the geographic distribution of air masses 36 h prior to the collection of a rain event in Bermuda (Figure 1). During the warm season (April to September), when the Bermuda-Azores High pressure system sets in, almost all events originate over the ocean, with a mixture of events coming primarily from the south, from both southeast and southwest of the island (Figure 1b). During the cool season (October to March), the Bermuda-Azores High breaks down, and there is an almost equal number of events originating over the ocean and over the continental United States ($n = 25$ versus $n = 32$, respectively; Figure 1a). The events with air mass back trajectories that originate over the continental United States (Figure S1) tend to travel much faster and therefore much farther than events that originate over the ocean (Figure S2). Due to the variability in air mass source region during the cool season, season alone is an inadequate metric of air mass origin. Thus, the data are analyzed in terms of both the season of collection and the air mass source, which will be distinguished as marine air mass back trajectory (AMBT) for the air masses that originate over the ocean and continental AMBT for air masses that originate from the continental United States 36 h prior to arriving at Bermuda. Those few samples that had AMBT origins on the coast of the United States are classified as coastal AMBT to avoid bias in assigning them to either marine or continental AMBT categories.

3.2. Ammonium Concentrations

Inorganic N (NH₄⁺ + NO₃[−]) constituted 57–100% of total N in Bermuda rainwater, with an average of 87% across all rain samples. There were 98 rainwater samples collected between 1 September 2009 and 9 August 2011 that were analyzed for ammonium concentrations and isotopes (discussed below). The NH₄⁺ concentrations ranged from 2.1 to 24.6 μM, with a numerical average of 7.3 ± 4.7 μM. For the different AMBT regimes, the NH₄⁺ concentrations ranged from 2.1 to 18.6 μM for the marine AMBT ($n = 57$), 2.3 to 24.6 μM for the continental AMBT ($n = 37$), and 5.2 to 14.4 μM for the coastal AMBT ($n = 4$). The volume-weighted average NH₄⁺ concentration was 6.0 ± 4.2 μM for marine AMBT, 5.9 ± 3.2 μM for continental AMBT, and 7.8 ± 3.0 μM for coastal AMBT (Table 1).

There were additional 35 rainwater samples collected during this time frame with an NH₄⁺ concentration less than 2.0 μM, which is the lower limit for δ¹⁵N-NH₄⁺ isotope analysis using this method, and they are therefore not included in the isotope data set. Including the samples below 2.0 μM, the ammonium concentrations ranged from 0.36 to 24.6 μM with a numerical average of 6.2 ± 5.7 μM and a volume-weighted average of 4.1 ± 3.9 μM. For the different AMBT regimes, the NH₄⁺ concentrations ranged from 0.36 to 18.6 μM for the marine AMBT ($n = 80$), 0.96 to 24.6 μM for the continental AMBT ($n = 47$), and 1.3 to 15.8 μM for the coastal AMBT ($n = 5$). The volume-weighted average NH₄⁺ concentration was 3.5 ± 3.8 μM for marine AMBT, 5.4 ± 4.1 μM for continental AMBT, and 6.3 ± 5.7 μM for coastal AMBT.

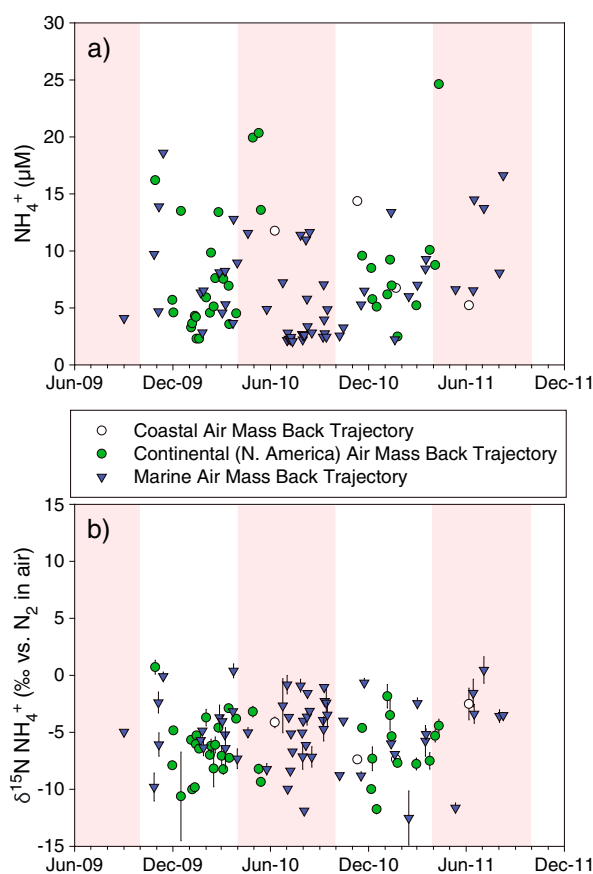


Figure 2. (a) Ammonium concentration (μM) and (b) $\delta^{15}\text{N}$ of NH_4^+ (‰ versus atmospheric N_2 in air) in rain samples collected on Bermuda between July 2009 and October 2011. The pink panels correspond to the warm season (April to September) while the white panels correspond to the cool season (October to March). Error bars denote the standard deviation of replicate isotopic measurements. Where error bars are not visible the standard deviation is smaller than the size of the marker.

the continental AMBT averaging $-6.4 \pm 2.6\text{‰}$ and the marine AMBT averaging $-4.9 \pm 3.0\text{‰}$. The mass-weighted continental AMBT average $\delta^{15}\text{N-NH}_4^+$ of $-5.8 \pm 2.5\text{‰}$ is also significantly lower than the marine AMBT mass-weighted average $\delta^{15}\text{N-NH}_4^+$ of $-4.1 \pm 2.6\text{‰}$ (Welch's unpaired t test, 95%, $p < 0.05$). If the data are binned by cool and warm seasons instead of back trajectory, the cool season average $\delta^{15}\text{N-NH}_4^+$ was $-6.0 \pm 2.8\text{‰}$ ($n = 59$) and the warm season average $\delta^{15}\text{N-NH}_4^+$ was $-4.6 \pm 2.8\text{‰}$ ($n = 39$), and they are statistically different (independent t test, 95%, $p = 0.02$). The cool season mass-weighted average $\delta^{15}\text{N-NH}_4^+$ was $-5.7 \pm 2.7\text{‰}$, and the warm season mass-weighted average $\delta^{15}\text{N-NH}_4^+$ was $-3.7 \pm 2.3\text{‰}$ (independent t test, 95%, $p = 0.0002$). If the data are binned by both AMBT and season, the marine AMBT warm season mass-weighted average $\delta^{15}\text{N-NH}_4^+$ is statistically different than the other averages (Table 2 and Figure S3).

4. Discussion

4.1. Rainwater Ammonium $\delta^{15}\text{N}$

In contrast to NO_3^- , the NH_4^+ concentrations in rainwater do not vary as a function of season or AMBT, nor does there appear to be a relationship with air temperature or the seasonality of biological activity in the surface ocean. There are statistically significant differences in the average $\delta^{15}\text{N-NH}_4^+$ for continental versus marine AMBT and for warm versus cool seasons (Figures 2b and S3), but the changes are much smaller than for $\delta^{15}\text{N-NO}_3^-$ [Altieri *et al.*, 2013; Hastings *et al.*, 2003], and there is not a clear pattern with AMBT or season. The lack of a strong dependence of concentration or $\delta^{15}\text{N-NH}_4^+$ on AMBT is arguably surprising. The

With or without the 35 samples with NH_4^+ concentrations below $2.0 \mu\text{M}$, the concentration of NH_4^+ does not vary significantly as a function of season (cool versus warm) or AMBT (marine versus continental versus coastal), and the populations are not statistically different (Figure 2a). In Bermuda rainwater measured from 1980 to 1984, and from 2007 to 2009, annual volume-weighted average ammonium concentrations ranged from 2 to $4 \mu\text{M}$, with no significant trends associated with air mass history [Keene *et al.*, 2014, and references therein]. In the same Bermuda rainwater samples analyzed by Hastings *et al.* [2003], the volume-weighted average concentration of reduced N ($\text{NH}_4^+ + \text{WSON}$) was not statistically different from the warm season ($6.4 \mu\text{M}$) to the cool season ($7.5 \mu\text{M}$) [Knapp *et al.*, 2010].

3.3. N Isotopes of Ammonium

The measurements of $\delta^{15}\text{N-NH}_4^+$ in Bermuda rain ranged from -12.5 to 0.7‰ from 1 September 2009 to 9 August 2011 (Figure 2b), with a numerical average of $-5.5 \pm 2.9\text{‰}$ (Table 1 and Figure 2b). The $\delta^{15}\text{N-NH}_4^+$ does not correlate with $[\text{NH}_4^+]$, $[\text{nss-SO}_4^{2-}]$, $[\text{NO}_3^-]$, $\delta^{15}\text{N-NO}_3^-$, $\delta^{18}\text{O-NO}_3^-$, or rainfall amount (not shown). The mean $\delta^{15}\text{N-NH}_4^+$ for the different AMBT are significantly different (independent t test, 95%, $p < 0.05$), with

Table 2. The Average ± 1 SD (n) Concentrations and Isotopic Ratios of N in Rainwater Ammonium Binned by Both the Season (Cool and Warm) and the Source Region of the Events AMBT (Marine, Continental, or Coastal)^a

	Continental AMBT Cool Season	Continental AMBT Warm Season	Marine AMBT Cool Season	Marine AMBT Warm Season
^b [NH ₄ ⁺] (μM)	5.37 ± 2.23 (32)	11.70 ± 6.08 (5)	6.20 ± 3.34 (25)	5.89 ± 4.70 (32)
^c δ ¹⁵ N NH ₄ ⁺ (‰)	-5.9 ± 2.6	-5.4 ± 1.4	-5.2 ± 2.6	-3.3 ± 2.4
^d δ ¹⁵ N NH ₄ ⁺ (‰)	-6.4 ± 2.7	-6.1 ± 2.6	-5.2 ± 3.0	-4.6 ± 3.0

^aThe number of samples measured for ammonium concentrations and isotopes in each category is in parentheses.

^bVolume-weighted average.

^cMass-weighted average.

^dNumerical average.

anthropogenic NH₃ emissions over the continental United States due to agriculture, animal husbandry, and fossil fuel combustion are all estimated to be much larger than the oceanic NH₃ source [Erismann *et al.*, 2007].

The lack of a large trajectory or seasonal trend in δ¹⁵N-NH₄⁺ could be due to (1) year-round domination by continental/anthropogenic sources that persists even when AMBT regimes shift, (2) seasonal and trajectory-based changes in sources or processes that coincidentally yield the same isotopic signature, or (3) year-round domination of the NH₄⁺ in Bermuda rainwater by a local marine source.

The first hypothesis is not supported by the concentration data and the known lifetimes of NH_{3(g)} and NH₄⁺_(p). Similar to NO₃⁻, the concentration of NH₄⁺ in Bermuda rainwater, regardless of season or trajectory, was much lower than in rainwater collected in the United States. The concentration of NH₄⁺ in weekly rainwater collections in the eastern United States from October to March, 2009–2011, ranged from 0.3 to 221 μM with an average of 13.2 ± 16.8 μM [National Atmospheric Deposition Program, 2007], compared to a range of 0.4 to 28.2 μM and an average of 6.2 ± 5.7 μM for Bermuda rain. Ammonia gas has a much shorter lifetime than NH₄⁺ aerosols (hours versus days, respectively) [Xu and Penner, 2012]; therefore, if an anthropogenic source of NH₄⁺ is persisting in Bermuda all year, it must be from longer lived fine mode ammonium aerosol particles. The continental AMBT travels quite far in 36 h, whereas the marine AMBT tend to stagnate near Bermuda (Figures 1, S1, and S2). If the marine AMBT are extended to 72 h, to better approximate the longer lifetime of ammonium sulfate particles, they still do not reach the continental United States (Figure S4). With a lifetime of days, and no apparent pathway for transport from North America, it seems unlikely that continental/anthropogenic ammonium aerosols are persisting in the marine atmosphere during the entire warm season when the Bermuda-Azores High pressure system is present.

Ammonia emissions in the United States are lowest during January and February, increase significantly during March, and remain high until October [Pinder *et al.*, 2006]. As a result, we might expect to see distinct isotopic changes at Bermuda from the time period of December–February when emissions in the United States are low to the transition months of March and September when air masses still frequently come from North America but ammonia emissions are much higher. This pattern is not observed, which suggests that our results are not heavily influenced by emissions from the United States. The second hypothesis requires atmospheric processing reactions to selectively influence NH₄⁺ in continental air masses, and not marine air masses, such that as NH₄⁺ is lost during transport from North America; the continental NH₄⁺ is left with a concentration and δ¹⁵N coincidentally similar to that measured from marine air masses. When fine mode anthropogenic NH₄NO₃ aerosols encounter marine air, there is essentially complete dissociation to NH₃ and HNO₃; therefore, there would be no expression of any isotope effect associated with dissociation, and the NH₃ should have an isotopic composition similar to its original source, likely from volatilization. The NH₃ will then react with sulfate to form ammonium sulfate aerosols. There is one estimate of the equilibrium isotope effect associated with the formation of ammonium sulfate aerosols from a laboratory experiment, which reported a value of 33‰ [Heaton *et al.*, 1997]. This would result in high δ¹⁵N particles, which is supported by measurements of particle δ¹⁵N over the continents. The total N in PM₁₀ aerosols in India, comprised primarily of NH₄⁺ (78%), had a δ¹⁵N ranging from 15.7 to 31.2‰, which the authors attributed to animal excreta and biomass burning in Southeast Asia [Pavuluri *et al.*, 2010]. The aerosol δ¹⁵N-NH₄⁺_(p) measured in a rural area of Japan ranged from 1.3 to 38.5‰ with an average of 16.1‰, and these high values were also attributed to agricultural sources such as animal waste and fertilizer [Kawashima and Kurahashi, 2011]. Since continental

aerosol $\delta^{15}\text{N-NH}_4^+(\text{p})$ is high in $\delta^{15}\text{N}$, there would have to be a preferential loss of $^{15}\text{N-NH}_4^+(\text{p})$ during transport to Bermuda for the rainwater to have low $\delta^{15}\text{N-NH}_4^+$ during the continental AMBT. The primary loss process for NH_4^+ aerosols during transport is wet deposition. It has been suggested that $\delta^{15}\text{N}$ declines progressively in consecutive low volume rain events due to an equilibrium fractionation in the dissolution of NH_3 that preferentially incorporates $^{15}\text{N-NH}_3$ in initial rain events [Heaton, 1987]. However, other studies in polluted regions have found no trend on consecutive days [Jia and Chen, 2010; Zhang et al., 2008], and there is evidence that the incorporation of NH_3 into rainwater is not controlled by traditional solubility theory or Henry's Law [Ayers et al., 1984]. To our knowledge, there are no studies that show isotopic fractionation during precipitation scavenging of NH_4^+ aerosols. In Bermuda rainwater, there is no distinct pattern in $\delta^{15}\text{N-NH}_4^+$ for consecutive rain events, suggesting that fractionation from dissolution is not a major driver of the measured isotopic variation (Figure 2). There is also no relationship between the distance an air mass has traveled and rainwater $\delta^{15}\text{N-NH}_4^+$. The lack of difference in the concentration or $\delta^{15}\text{N-NH}_4^+$ in rainwater between fast moving continental AMBT and slow moving marine AMBT in Bermuda, combined with the high $\delta^{15}\text{N-NH}_4^+(\text{p})$ associated with continental/anthropogenic ammonium sulfate aerosols, argues against the second hypothesis.

The third hypothesis, that a marine source of NH_4^+ is important year round, is supported by changes in the $\delta^{15}\text{N}$ of aerosol NH_4^+ from the polluted coastal environment to the open ocean. The aerosol $\delta^{15}\text{N-NH}_4^+(\text{p})$ was higher in air masses that originated over the continent ($6 \pm 6\text{‰}$) than in air masses that originated over the ocean ($-9 \pm 8\text{‰}$), and samples as low as -11‰ collected on a ship were observed in the Eastern Atlantic Ocean 200 km offshore [Yeatman et al., 2001]. This trend is supported by aerosol $\delta^{15}\text{N-NH}_4^+(\text{p})$ measurements made in a transect from the UK to the Falklands where higher concentrations of aerosol NH_4^+ had higher $\delta^{15}\text{N}$, attributed to terrestrial/continental sources, and lower concentrations of aerosol NH_4^+ had lower $\delta^{15}\text{N}$, attributed to a remote marine source [Jickells et al., 2003]. The decrease in $\delta^{15}\text{N-NH}_4^+(\text{p})$ from polluted to marine regions, combined with the measured Bermuda rainwater $\delta^{15}\text{N-NH}_4^+$, with all but four samples less than 0‰ , supports the hypothesis that the ocean is a local NH_3 source that contributes low $\delta^{15}\text{N-NH}_4^+$ to marine rainwater. Indeed, in the remote South Pacific, significant correlation was found between concentrations of NH_4^+ and methanesulfonic acid in rainwater, similarly suggesting an oceanic NH_4^+ source [Jung et al., 2011]. In previous work on rainwater concentrations at Bermuda, the potential influence of the island itself as a local source was explored and discounted as negligible [Moody and Galloway, 1988]. Consistent with this interpretation, there was no relationship between the ammonium concentration and $\delta^{15}\text{N}$, which would be expected if high concentration events were due to local NH_3 sources.

4.1.1. Atmospheric Ammonium Isotope Model

To test the hypothesis that ocean emissions of NH_3 could be the dominant source of NH_4^+ measured in marine rainwater, a box model was developed of the concentrations and isotopic composition of NH_4^+ and NH_3 in seawater ($\text{NH}_4^+(\text{sw})$ and $\text{NH}_3(\text{sw})$), ammonia gas and ammonium particles ($\text{NH}_3(\text{g})$ and $\text{NH}_4^+(\text{p})$) in the overlying atmosphere, and the NH_4^+ in rain (Figure 3a). The initial conditions and default parameter values of the box model were selected to represent typical conditions in the subtropical North Atlantic ocean and atmosphere around Bermuda (Table S2), and the model was run from these initial conditions forward in time until a steady state was reached. The model was initialized with surface ocean NH_x of a given concentration and isotopic composition, and the response of the atmospheric $\text{NH}_3(\text{g})$ and $\text{NH}_4^+(\text{p})$ pools was investigated. The air-sea flux was simulated explicitly using the thin film model [Johnson and Bell, 2008; Johnson et al., 2008; Liss and Slater, 1974], while the rates of gas-to-particle conversion and dry and wet deposition were parameterized.

The surface ocean concentration of NH_x is typically very low in the Sargasso Sea, $\sim 5\text{--}50\text{ nM}$ [Fawcett et al., 2014; Lipschultz, 2001], which has precluded the direct measurement of its $\delta^{15}\text{N}$. Previous work indicates that the $\delta^{15}\text{N-NH}_4^+$ produced into Sargasso Sea surface waters is low (-4 to -1‰) [Fawcett et al., 2011; Knapp et al., 2011], which is largely the consequence of isotope fractionation associated with metabolic NH_4^+ production [Checkley and Miller, 1989; Macko et al., 1986; Silfer et al., 1992], coupled with the production of dissolved organic nitrogen and sinking organic matter with high $\delta^{15}\text{N}$ [Altabet, 1988; Knapp et al., 2011]. To represent these conditions, the ocean NH_x pool in the model was set to 20 nM and -2‰ .

There is great variability reported in $\delta^{15}\text{N-NH}_3(\text{g})$ measured over the continents, -20 to $+25\text{‰}$, which seems to be related to the proximity of the source [Freyer, 1978; Moore, 1977]. To our knowledge, there are no $\delta^{15}\text{N}$ measurements of the $\text{NH}_3(\text{g})$ emitted from the ocean. As depicted in Figure 3a, the $\delta^{15}\text{N-NH}_3(\text{g})$ emitted from the ocean should depend on the initial $\delta^{15}\text{N}$ of the NH_x pool in seawater, the distribution and equilibrium

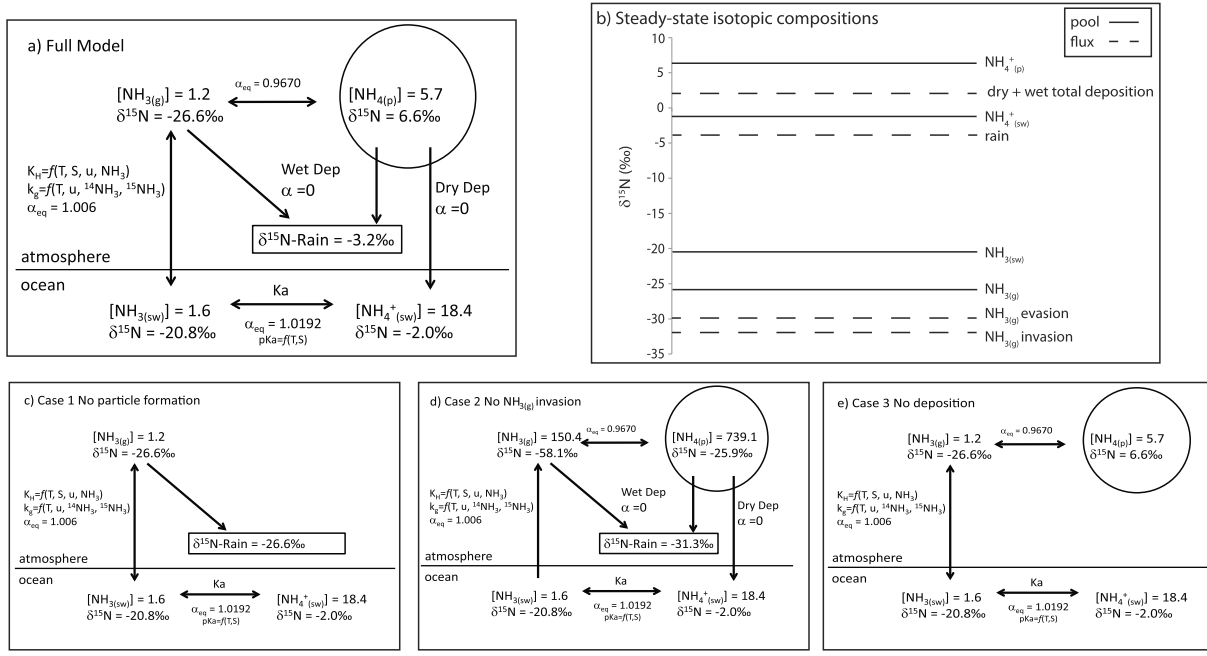


Figure 3. Schematics for the steady state box model showing the fluxes and isotope effects of ammonium and ammonia in seawater ($\text{NH}_4^+(\text{sw})$ and $\text{NH}_3(\text{sw})$), ammonia gas and ammonium particles ($\text{NH}_3(\text{g})$ and $\text{NH}_4^+(\text{p})$) in the atmosphere, and the resulting rainfall. The concentrations and $\delta^{15}\text{N}$ values for the (a) standard full model case, and (b) the resulting $\delta^{15}\text{N}$ values for all steady state pools and fluxes from the full model. The end-member cases are also shown, (c) with no particle formation, (d) the end-member case where $\text{NH}_3(\text{g})$ invasion is prohibited, and (e) the end-member case where there is no atmospheric deposition. The concentrations of $\text{NH}_3(\text{g})$ and $\text{NH}_4^+(\text{p})$ are in nmol m^{-3} , and $\text{NH}_4^+(\text{sw})$ and $\text{NH}_3(\text{sw})$ concentrations are in nM.

deprotonation isotope effect of NH_x to $\text{NH}_4^+(\text{sw})$ and $\text{NH}_3(\text{sw})$, and the isotope effects associated with the volatilization of $\text{NH}_3(\text{sw})$ to $\text{NH}_3(\text{g})$. At a typical surface ocean pH of 8.2, 92% of the NH_x is as $\text{NH}_4^+(\text{sw})$ and 8% is as $\text{NH}_3(\text{sw})$. The equilibrium fractionation factor of deprotonation ($\alpha_{\text{NH}_4^+(\text{sw}) - \text{NH}_3(\text{sw})}$), where $\alpha_{\text{NH}_4^+(\text{sw}) - \text{NH}_3(\text{sw})} = R_{\text{NH}_4^+(\text{sw})}/R_{\text{NH}_3(\text{sw})} = (^{15}\text{NH}_4^+(\text{sw})/^{14}\text{NH}_4^+(\text{sw})) / (^{15}\text{NH}_3(\text{sw})/^{14}\text{NH}_3(\text{sw}))$, is 1.0192 [Hermes et al., 1985]. This results in a low $\delta^{15}\text{N}$ - $\text{NH}_3(\text{sw})$ pool that is available for emission to the atmosphere. In addition, the isotope discriminations associated with air/sea gas exchange are such that low $\delta^{15}\text{N}$ - NH_3 is preferentially released into the atmosphere. First, there is an equilibrium fractionation factor associated with NH_3 efflux ($\alpha_{\text{NH}_3(\text{sw}) - \text{NH}_3(\text{gas})} = 1.006$) [Kirshenbaum et al., 1947; Thode et al., 1945; Urey, 1947]. Second, the kinetics also favors low ^{14}N - NH_3 efflux. In the thin film model, the flux of $\text{NH}_3(\text{sw})$ out of the ocean is dependent on the air/sea gas transfer velocity (k_g) and the Henry's law constant (K_H). We explicitly calculated the molecular weight dependent k_g and the temperature and salinity corrected K_H using the numerical scheme from Johnson [2010]. The differing k_g values for $^{14}\text{NH}_3$ and $^{15}\text{NH}_3$ result in a kinetic isotope effect of 1.003. The net effect, then, is that the $\text{NH}_3(\text{g})$ emitted from the surface ocean is 6–9‰ lower in $\delta^{15}\text{N}$ than the $\text{NH}_3(\text{sw})$.

Once in the atmosphere, NH_3 is redeposited as one of two forms, with very different isotopic effects. Ammonium sulfate particles form with an equilibrium fractionation factor that is apparently large ($\alpha_{\text{NH}_3(\text{gas}) - \text{NH}_4^+(\text{part})} = 0.9670$) [Heaton et al., 1997], elevating the $\delta^{15}\text{N}$ of $\text{NH}_4^+(\text{p})$ relative to the atmospheric $\text{NH}_3(\text{g})$ pool. The partitioning of atmospheric NH_x between $\text{NH}_3(\text{g})$ and $\text{NH}_4^+(\text{p})$ and thus their relative contribution to $\text{NH}_4^+(\text{p})$ in rainfall has a major effect on the $\delta^{15}\text{N}$ of atmospheric NH_x and rain $\delta^{15}\text{N}$ - NH_4^+ , which is discussed in detail below. In the model, particle dry deposition and wet deposition are assumed to have no significant isotope fractionation.

4.1.2. Model Results

In order to investigate the conditions under which low $\delta^{15}\text{N}$ - NH_4^+ in precipitation is generated in the marine atmosphere, we step through a suite of model runs representing end-member scenarios (Figures 3c–3e). The first case eliminates particle formation and only allows deposition of $\text{NH}_3(\text{g})$. This case is most similar to a pure equilibrium case with the equilibration of $\text{NH}_4^+(\text{sw})$ with $\text{NH}_3(\text{sw})$ and of $\text{NH}_3(\text{sw})$ with $\text{NH}_3(\text{g})$ (i.e., $\text{NH}_4^+(\text{sw}) \longleftrightarrow \text{NH}_3(\text{sw}) \longleftrightarrow \text{NH}_3(\text{g})$, Figure 3c). The distribution of $\text{NH}_3(\text{sw})$ and $\text{NH}_4^+(\text{sw})$ is driven by the

pKa of NH_4^+ in seawater, the pH of the surface ocean, and the equilibrium isotope effect of deprotonation (1.0192). This results in a large NH_4^+ (sw) pool (18.4 nM) with a $\delta^{15}\text{N}$ of -2.0‰ and a small NH_3 (sw) pool (1.6 nM) with a $\delta^{15}\text{N}$ of -20.8‰ . The small NH_3 (sw) pool is available for gas exchange with the atmosphere, which is driven by the K_H and k_g of NH_3 and the equilibrium isotope effect of exchange (1.006). The NH_3 (g) pool is 1.2 nmol m^{-3} with a $\delta^{15}\text{N}$ of -26.6‰ . Therefore, without any particle formation, in the equilibrium case the small amount of rainwater NH_4^+ deposited from the marine atmosphere would be very low in $\delta^{15}\text{N}$ as it would be similar to the NH_3 (g) pool fluxing into the surface ocean.

In the second case, particle formation and deposition to the ocean is added, while the flux of NH_3 (g) back to the ocean via invasion is prevented (i.e., NH_4^+ (sw) \longleftrightarrow NH_3 (sw) \rightarrow NH_3 (g) \longleftrightarrow NH_4^+ (p) \rightarrow NH_4 (sw), Figure 3d). The amount and $\delta^{15}\text{N}$ of the NH_3 (sw) and NH_4^+ (sw) are not impacted, but the NH_3 (g) pool increases to $150.4 \text{ nmol m}^{-3}$ with a $\delta^{15}\text{N}$ of -58.1‰ , and the NH_4^+ (p) is $739.1 \text{ nmol m}^{-3}$ with a $\delta^{15}\text{N}$ of -25.9‰ . With the invasion of NH_3 (g) precluded, the $\delta^{15}\text{N}$ - NH_4^+ of all deposition (rain + dry deposition) must come to equal the $\delta^{15}\text{N}$ of gross NH_3 evasion from the ocean; and, indeed, both have a $\delta^{15}\text{N}$ of -29.9‰ . The rainwater flux alone has a $\delta^{15}\text{N}$ - NH_4^+ of -31.3‰ . Therefore, if the ocean flux of ammonia is unidirectional (i.e., only out of the ocean), the low $\delta^{15}\text{N}$ - NH_4^+ (p) would lead to rainwater $\delta^{15}\text{N}$ - NH_4^+ much lower than what we observe.

In the third case, the flux of NH_3 (g) is returned to bidirectional, particle formation is included, but no deposition is allowed (i.e., NH_4^+ (sw) \longleftrightarrow NH_3 (sw) \longleftrightarrow NH_3 (g) \longleftrightarrow NH_4^+ (p), Figure 3e). The concentration and $\delta^{15}\text{N}$ of the seawater pools are not affected, the NH_3 (g) is 1.2 nmol m^{-3} with a $\delta^{15}\text{N}$ of -26.6‰ , and the particle pool is 5.8 nmol m^{-3} with a $\delta^{15}\text{N}$ of 6.6‰ , which is driven by the large equilibrium isotope effect of ammonium sulfate particle formation (0.9670). This is similar to the full model case, as deposition to the ocean is nonfractionating in our model. The $\delta^{15}\text{N}$ of the rainwater flux to the ocean would range from -15.6 to 1.0‰ , depending on assumed scavenging efficiencies, similar to the full model. The relatively good fit of this end-member case to the data implies that the gas exchange driven influx of NH_3 (g) into the ocean is critical in offsetting the low $\delta^{15}\text{N}$ - NH_3 (sw) efflux, allowing the $\delta^{15}\text{N}$ of NH_x in the atmosphere to be adequately high to generate NH_4^+ (p) with the high $\delta^{15}\text{N}$ needed to drive the precipitation NH_x flux to a $\delta^{15}\text{N}$ between -10 and 0‰ . A further implication is that the ocean NH_x fluxes are dominated by gas exchange equilibration, including both evasion and invasion of NH_3 , with the rainfall NH_4^+ flux representing a small, high $\delta^{15}\text{N}$ fraction of total NH_x flux back to the ocean. As a result, even if the rain is highly effective at removing NH_3 (g) and NH_4^+ (p), the rainfall NH_4^+ flux will still be a small, high $\delta^{15}\text{N}$ - NH_x flux.

The full model is the same as the third case above, but with both NH_3 (g) and NH_4^+ (p) being deposited to the ocean through dry and wet deposition (Figure 3a). The modeled sea to air flux is $9.8 \text{ pmol m}^{-2} \text{ s}^{-1}$ at a wind speed of 11 m s^{-1} , the average wind speed overall sample days as measured by the Bermuda Weather Service. This is consistent with measurements of the sea to air flux at $\sim 30^\circ\text{N}$, which was estimated to be around $\sim 10 \text{ pmol m}^{-2} \text{ s}^{-1}$ [Johnson *et al.*, 2008]. The modeled NH_3 (g) concentration is 1.2 nmol m^{-3} , and the NH_4^+ (p) concentration is 5.7 nmol m^{-3} , which is the same order of magnitude as previous measurements at Bermuda ($\text{NH}_3 = 1\text{--}5 \text{ nmol m}^{-3}$ and NH_4^+ (p) = $12\text{--}15 \text{ nmol m}^{-3}$) [Johnson *et al.*, 2008]. The modeled $\delta^{15}\text{N}$ - NH_3 (g) is -26.9‰ , and the $\delta^{15}\text{N}$ - NH_4^+ (p) is 6.3‰ (Figure 3b).

The NH_3 air/sea flux is controlled by the pKa and K_H , which are both temperature dependent, and the k_g , which is temperature and wind speed dependent. Because the concentration of NH_4^+ (p) is dependent on the NH_3 (g) concentration, it in turn has a temperature sensitivity. However, the NH_3 (g)/ NH_4^+ (p) partitioning itself is not very sensitive to temperature. As a result, the concentration of NH_3 (g) and NH_4^+ (p) is sensitive to temperature and wind speed (Figure 4a), while the $\delta^{15}\text{N}$ - NH_3 (g) and $\delta^{15}\text{N}$ - NH_4^+ (p) is primarily dependent on the k_g and therefore sensitive only to wind speed (Figure 4b).

Assuming wet removal through rainfall has 100% efficiency with respect to NH_3 (g) and 10 to 100% efficiency with respect to NH_4^+ (p), the calculated rainwater $\delta^{15}\text{N}$ - NH_4^+ would range from -15.9 to 0.7‰ , respectively. These values are very similar to the $\delta^{15}\text{N}$ - NH_4^+ of the Bermuda rainwater measurements, which ranged from -12.5 to 0.7‰ with an average of -5.5‰ . Assuming 25 to 100% scavenging of the NH_4^+ (p) results in a 55 to 83% contribution of NH_4^+ (p) to the total concentration of rainwater NH_4^+ , this is consistent with previous estimates, which range from 60 to 90% [Mészáros and Szentimrei, 1985; Shimshock and De Pena, 1989]. Measurements of the rain scavenging ratios for NH_3 (g) and NH_4^+ (p) are difficult due to the difficulties in accurately measuring ambient NH_3 (g) concentrations, however, large

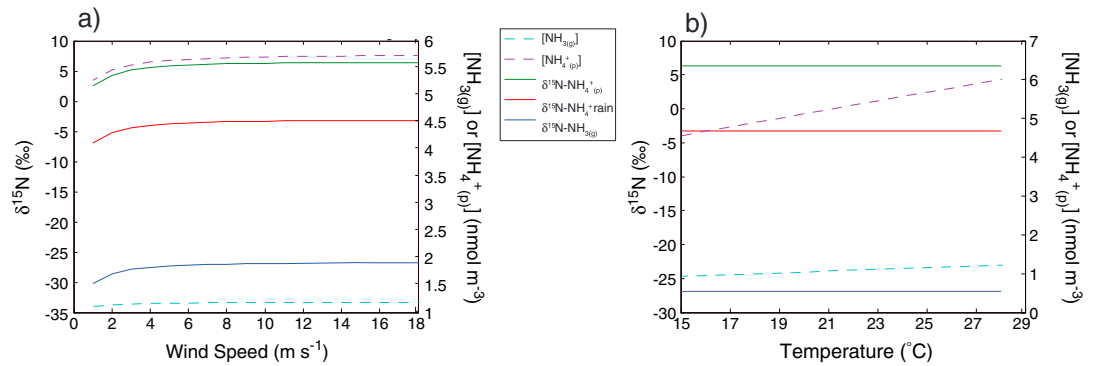


Figure 4. Sensitivity analysis of the impact of (a) wind speed and (b) temperature on the concentration of $\text{NH}_3(\text{g})$ and $\text{NH}_4^+(\text{p})$ (right axis, dashed lines), and the isotopic composition of $\delta^{15}\text{N-NH}_3(\text{g})$, $\delta^{15}\text{N-NH}_4^+(\text{p})$, and the $\delta^{15}\text{N-NH}_4^+$ in rain (left axis, solid lines).

variations (orders of magnitude) have been observed in daily scavenging ratios [Kasper-Giebl et al., 1999]; thus, we allow for a large range in the model.

The Sargasso Sea near Bermuda is considered an N limited region of the ocean, with only hundredths to several tenths of a micromolar ammonium in the upper ~100 m [Lipschultz, 2001]; thus, it is in some ways counterintuitive that the surface ocean could be the source for the ammonium in Bermuda rain, the concentration of which is typically 5 μM . It might seem even more surprising that the dominant return mechanism of this N to surface waters could be the dissolution of atmospheric ammonia into sea water and not the rainfall flux itself. Nevertheless, the ammonium/a concentration and $\delta^{15}\text{N}$ data and their consistency with our simple box model support this picture as applicable throughout the year, regardless of air mass history. In essence, our data speak to the efficient kinetics of ammonia evasion from surface seawater, leading atmospheric ammonia to accumulate in the atmosphere to the extent that NH_3 evasion and invasion reach steady state.

The average $\delta^{15}\text{N-NH}_4^+$ for marine AMBT is slightly higher than continental AMBT (Table 1), and the warm season average is also slightly higher than the cool season average. However, the changes are smaller and in the opposite direction than might be expected from an anthropogenic influence during continental AMBT or the cool season. The model was run under cool season and warm season scenarios (Figure 5b). Temperature and wind speed were set based on averages from cool and warm seasons data collected

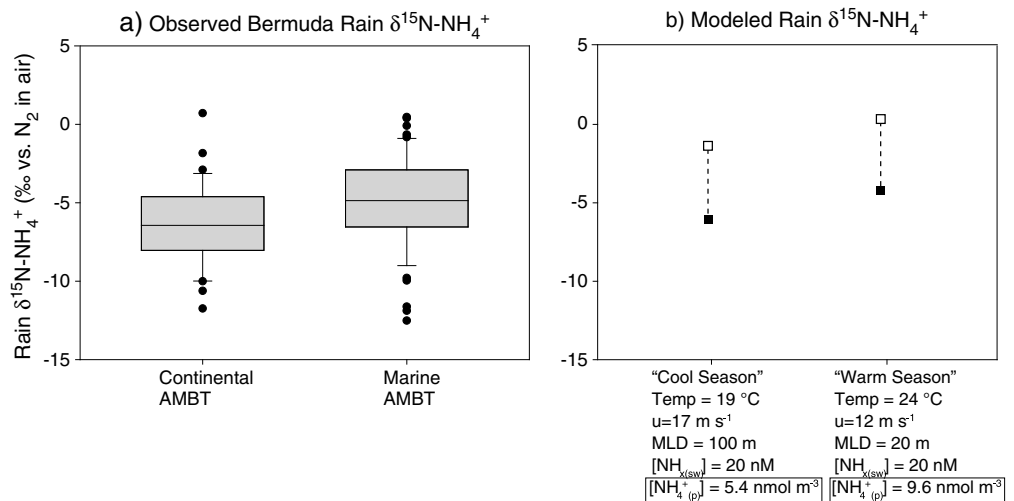


Figure 5. (a) Box and whisker plot of rainwater $\delta^{15}\text{N-NH}_4^+$ data from Bermuda as a function of continental and marine AMBT compared to (b) the model output for the cool season and warm season scenarios. The vertical dashed lines indicate the range in model output values for the rain water $\delta^{15}\text{N-NH}_4^+$ assuming a range of scavenging efficiencies. The open squares indicate an upper bound of 100% scavenging of $\text{NH}_3(\text{g})$ and $\text{NH}_4^+(\text{p})$, and the filled squares indicate 100% scavenging of $\text{NH}_3(\text{g})$ and 50% scavenging of $\text{NH}_4^+(\text{p})$.

over the same time period as the samples analyzed here. The average temperature and wind speed for the cool season was 19°C and 17 m s⁻¹ while the warm season averages were 24°C and 12 m s⁻¹ (data from Bermuda Weather Service; www.weather.bm). For surface ocean mixed layer depth, we used climatological means (100 and 20 m for the cool and warm seasons, respectively) [Lomas *et al.*, 2013]. The measured concentration of NH₄⁺_(p) is slightly higher in the warm season (Table S3), likely due to an increased contribution from long-range transport of dust particles from the Sahara and the increased flux of NH_{3(g)} due to higher temperatures, as discussed in Johnson *et al.* [2008].

A box and whisker plot of the rainwater observations (Figure 5a) are compared to the model output for the two scenarios (Figure 5b). A range in model output δ¹⁵N-NH₄⁺ is shown which corresponds to a range in scavenging efficiencies. The upper estimate (open squares; Figure 5b) represents 100% scavenging of NH_{3(g)} and NH₄⁺_(p), and the lower estimate (filled squares; Figure 5b) represents 100% scavenging of NH_{3(g)} and 50% scavenging of NH₄⁺_(p). The model scenarios reproduce the seasonal variability in the data with the warm season having slightly higher δ¹⁵N-NH₄⁺ rainwater than the cool season. Only ~0.15‰ of this change is due to the seasonal differences in wind speed, temperature, and mixed layer depth. The remainder of the seasonal difference in the model is due to the changes in aerosol concentration. In the warm season scenario, there is a larger contribution of high δ¹⁵N particles to the rainwater flux. The ability of the model to reproduce the slight seasonal shift in δ¹⁵N-NH₄⁺ seen in the data provides further support to the hypothesis that the ocean can be the dominant ammonium source throughout the year, regardless of changes in AMBT.

The day-to-day δ¹⁵N-NH₄⁺ variability is much larger than the changes with season or AMBT discussed above, and the full dynamic range is similar in both seasons (Figures 2b and 5a). This suggests that the dominant driver of δ¹⁵N-NH₄⁺ variation must operate on an event time scale. The variations in temperature at Bermuda are gradual over time, but changes in wind speed can be significant from day to day and may impact the δ¹⁵N-NH₄⁺ of a given rain event. Wind speeds around Bermuda can vary from 2 to 18 m s⁻¹, which will impact both the concentration and δ¹⁵N-NH_{3(g)} and δ¹⁵N-NH₄⁺_(p) (Figure 4a). At low wind speeds the rain δ¹⁵N-NH₄⁺ could be as low as -10.1‰, and at high wind speeds it can be as large as 0.85‰. These values are within the range for observations of δ¹⁵N-NH₄⁺ at Bermuda; and therefore, changes in wind speed could explain some of the day to day variability in δ¹⁵N-NH₄⁺ of rain at Bermuda.

The ratio of NH₄⁺ to nss-SO₄²⁻ also varies between rain events (Figure S5). All of the continental AMBT events fall below the 2:1 line and cluster around the 1:1 line, which indicates NH₄HSO₄ formation. The marine AMBT events are more variable and fall along both the 2:1 (NH₄)₂SO₄ and the 1:1 NH₄HSO₄ lines, with some events having NH₄⁺ to nss-SO₄²⁻ ratios above 2:1 indicating an excess of NH₃, as discussed in the supporting information. The average NH₄⁺ to nss-SO₄²⁻ ratio for continental AMBT is 0.90 ± 0.5 and for marine AMBT is 2.0 ± 3.2. The direction of the NH_x flux between NH_{3(g)} and NH₄⁺_(p) is determined by the difference in concentration between the NH_{3(g)} and the partial pressure of NH_{3(g)} over the aerosol [Johnson and Bell, 2008]. The partial pressure of NH_{3(g)} over the aerosol is controlled by the acidity, i.e., the nss-SO₄²⁻ concentration; and therefore, changes in acidity lead to either an increase or decrease in the uptake of NH_{3(g)} into the particle phase, with a compensating flux of NH_{3(g)} out of the ocean. However, as discussed by Johnson and Bell [2008], changes in the ratio of NH₄⁺_(p) to nss-SO₄²⁻_(p) are more important than the absolute concentrations. The parameterization of the rate constant of NH₄⁺_(p) formation from NH_{3(g)} in the model is similar to other values from the literature [e.g., Asman *et al.*, 1998], but it does not account for variations in nss-SO₄²⁻ concentration. By changing the rate constant for NH₄⁺_(p) formation such that the concentration ranges from 10 to 120 nmol m⁻³ (comparable to the dynamic range observed at Bermuda; Table S3), the resulting rain δ¹⁵N-NH₄⁺ can vary from -16.0 to 2.3‰, suggesting that this could indeed be the driver of event-to-event changes in rain δ¹⁵N-NH₄⁺. If the acidity were such that almost all NH_{3(g)} is converted to NH₄⁺_(p), then the equilibrium isotope effect from particle formation would be poorly expressed. This would result in the total remaining atmospheric NH_x pool having a δ¹⁵N of ~-26‰. Based on the model results, this suggests that there is a large equilibrium isotope effect for ammonium particle formation, such as that measured by Heaton *et al.* [1997], and that it is expressed in (i.e., elevates) the δ¹⁵N of NH₄⁺_(p), as a high δ¹⁵N of NH₄⁺_(p) is required to explain the observed rain δ¹⁵N-NH₄⁺. More explicit modeling of the aerosol dynamics, e.g., following the model of Johnson and Bell [2008], and more information on the isotope effects associated with uptake and neutralization would be needed to investigate the influence of NH₄⁺ to nss-SO₄²⁻ ratios and aerosol acidity on the aerosol formation processes and the resulting isotopic composition of NH₄⁺_(p).

5. Conclusions

In contrast to rainwater NO_3^- [Altieri *et al.*, 2013; Hastings *et al.*, 2003] and total reduced N [Knapp *et al.*, 2010], the NH_4^+ in rainwater does not have a clear concentration or $\delta^{15}\text{N}$ relationship with season or air mass history. A simple box model demonstrates that it is quantitatively feasible for the ocean to be the NH_4^+ source, reproducing the concentrations of $\text{NH}_3(\text{g})$ and $\text{NH}_4^+(\text{p})$ that are observed near Bermuda, the $\delta^{15}\text{N}$ of the resulting rainfall NH_4^+ , and the direction and magnitude of the small seasonal shifts in $\delta^{15}\text{N}-\text{NH}_4^+$. As a result, we propose that the subtropical North Atlantic Ocean could be the dominant source of atmospheric NH_3 and NH_4^+ in the lower atmosphere of the region throughout the year.

There has been debate as to whether the air-sea flux of ammonia has the time to attain equilibrium in the marine atmosphere, or if particle formation is too rapid, preventing equilibrium [Johnson and Bell, 2008; Johnson *et al.*, 2008; Quinn *et al.*, 1988, 1992, 1996]. When the flux out of the ocean is reduced, the dominant loss process of $\text{NH}_3(\text{g})$ is particle formation, while if the flux out of the ocean is increased, the dominant loss process is the exchange with the ocean, and equilibrium across the air-sea interface is attained. With very little flux out of the ocean, the $\delta^{15}\text{N}-\text{NH}_3(\text{g})$ is low due to particle formation, which has a large equilibrium isotope effect. This results in both low $\delta^{15}\text{N}-\text{NH}_3(\text{g})$ and low $\delta^{15}\text{N}-\text{NH}_4^+(\text{p})$ and would lead to $\delta^{15}\text{N}-\text{NH}_4^+$ values lower than observed in the Bermuda rainwater (case two above and Figure 3c). With a large flux, the concentration and $\delta^{15}\text{N}$ of $\text{NH}_3(\text{g})$ and $\text{NH}_4^+(\text{p})$ are higher, and more consistent with the concentrations and $\delta^{15}\text{N}-\text{NH}_4^+$ observed in Bermuda rainwater. This suggests that the air-sea flux of NH_3 does indeed achieve equilibrium between atmospheric and surface water NH_3 concentrations, and that the removal of atmospheric NH_x via rain is a relatively small gross flux when compared to air/sea exchange.

The dominant time scale of variation in rainwater $\delta^{15}\text{N}-\text{NH}_4^+$ at Bermuda is between events and days, with this variation largely overwhelming any seasonal changes. The model-derived sensitivities of the $\delta^{15}\text{N}$ of atmospheric $\text{NH}_3(\text{g})$ and $\text{NH}_4^+(\text{p})$ indicate that the range in observed rainwater $\delta^{15}\text{N}-\text{NH}_4^+$ at Bermuda, and in particular the event-to-event variability, could be due to the influence of changing wind speeds, which alters the relative rates of removal of atmospheric NH_x through dissolution and deposition.

The total amount of both anthropogenic and natural N deposition to the ocean remains poorly constrained due to a lack of observations. A recent review based on global N deposition modeling estimated that NH_x deposition to the ocean is 24 Tg N yr^{-1} with 87.5% from anthropogenic sources [Duce *et al.*, 2008]. This is a significant increase from preindustrial NH_x deposition, estimated to be 8 Tg N yr^{-1} with only 30% from anthropogenic sources. Bermuda is often downwind of a major pollution center and thus a site where the anthropogenic component of ammonium deposition should be apparent if it is globally important in terms of open ocean deposition.

Ammonium contributes 45% to the annual wet N deposition flux to Bermuda ($\text{NO}_3^- + \text{NH}_4^+ + \text{organic N}$). The wet flux of NH_4^+ from continental AMBT is very similar to the wet flux from marine AMBT (10.9 and $11.1 \text{ Tg N yr}^{-1}$). We have argued above that the NH_4^+ deposition with either marine or continental AMBT has isotopic properties suggesting that none of the NH_4^+ deposition requires a source other than the open ocean. The Duce *et al.* [2008] review suggests that 87.5% of NH_x deposition to the ocean is anthropogenic. Bermuda's position downwind of North America should be an ideal place to observe this. However, our results suggest that reduced nitrogen undergoes a dynamic cycling in the surface ocean and lower atmosphere and that the surface ocean cannot be considered a passive recipient of anthropogenic NH_x deposition. This interpretation of the data and its applicability to larger ocean regions will be effectively tested by comparable investigations of NH_x deposition in areas that are more remote from anthropogenic influence. In any case, extrapolation of this picture of Bermuda NH_x fluxes to the subtropical gyres in general implies that the anthropogenic component of atmospheric NH_x deposition to the open ocean, and thus the contribution of N deposition to the ocean's external N supply, is smaller than previously thought. Further studies are called for to explore the role of the surface ocean in the reactive N cycle of the marine atmosphere.

References

- Allen, A. G., R. M. Harrison, and J.-W. Erisman (1989), Field measurements of the dissociation of ammonium nitrate and ammonium chloride aerosols, *Atmos. Environ.*, 23(7), 1591–1599.
- Altabet, M. A. (1988), Variations in nitrogen isotopic composition between sinking and suspended particles: Implications for nitrogen cycling and particle transformation in the open ocean, *Deep Sea Res., Part A*, 35(4), 535–554.

Acknowledgments

This work was supported by NSF ATM-1044997 (to M.G.H., A.J.P. and D.M.S.), NSF OCE-1060947 (to D.M.S.), the Grand Challenges Program at Princeton University (to D.M.S.), and the NOAA Climate and Global Change Fellowship Program (to K.E.A.). The Tudor Hill facility is supported by NSF OCE-1130395. We thank B. Chang for collaborating on the ammonium isotope method adaptations; A. Marks and J. Rosset for sample collection assistance; R. Lauck, A. Gobel, and J. Garcia for analytical support; A. Buffen for helpful discussions on statistics; and J. Granger and A. Babbín for assistance in developing and coding the box model.

- Altieri, K. E., M. G. Hastings, A. R. Gobel, A. J. Peters, and D. M. Sigman (2013), Isotopic composition of rainwater nitrate at Bermuda: The influence of air mass source and chemistry in the marine boundary layer, *J. Geophys. Res. Atmos.*, *118*, 11,304–11,316, doi:10.1002/jgrd.50829.
- Asman, W. A. H., M. A. Sutton, and J. K. Schjorring (1998), Ammonia: Emission, atmospheric transport and deposition, *New Phytol.*, *139*(1), 27–48.
- Ayers, G. P., J. L. Gras, A. Adriaansen, and R. W. Gillett (1984), Solubility of ammonia in rainwater, *Tellus B*, *36B*(2), 85–91.
- Bohlke, J. K., C. J. Gwinn, and T. B. Coplen (1993), New reference materials for nitrogen-isotope-ratio measurements, *Geostand. NewsL.*, *17*(1), 159–164.
- Checkley, D. M., Jr., and C. A. Miller (1989), Nitrogen isotope fractionation by oceanic zooplankton, *Deep Sea Res., Part A*, *36*(10), 1449–1456.
- Clarisse, L., C. Clerbaux, F. Dentener, D. Hurtmans, and P.-F. Coheur (2009), Global ammonia distribution derived from infrared satellite observations, *Nat. Geosci.*, *2*, 479–483, doi:10.1038/ngeo551.
- Clegg, S. L., P. Brimblecombe, and A. S. Wexler (1998), Thermodynamic model of the system $\text{H}^+ - \text{NH}_4^+ - \text{SO}_4^{2-} - \text{NO}_3^- - \text{H}_2\text{O}$ at tropospheric temperatures, *J. Phys. Chem. A*, *102*(12), 2137–2154.
- Cornell, S. E., T. D. Jickells, J. N. Cape, A. P. Rowland, and R. A. Duce (2003), Organic nitrogen deposition on land and coastal environments: A review of methods and data, *Atmos. Environ.*, *37*(16), 2173–2191.
- Duce, R. A., et al. (2008), Impacts of atmospheric anthropogenic nitrogen on the open ocean, *Science*, *320*(5878), 893–897.
- Elliott, E. M., C. Kendall, S. D. Wankel, D. A. Burns, E. W. Boyer, K. Harlin, D. J. Bain, and T. J. Butler (2007), Nitrogen isotopes as indicators of NO_x source contributions to atmospheric nitrate deposition across the Midwestern and Northeastern United States, *Environ. Sci. Technol.*, *41*(22), 7661–7667.
- Elsler, J. J., T. Andersen, J. S. Baron, A.-K. Bergstrom, M. Jansson, M. Kyle, K. R. Nydick, L. Steger, and D. O. Hessen (2009), Shifts in Lake N:P stoichiometry and nutrient limitation driven by atmospheric nitrogen deposition, *Science*, *326*(5954), 835–837.
- Erisman, J. W., A. Bleeker, J. Galloway, and M. S. Sutton (2007), Reduced nitrogen in ecology and the environment, *Environ. Pollut.*, *150*(1), 140–149.
- Fawcett, S. E., M. W. Lomas, J. R. Casey, B. B. Ward, and D. M. Sigman (2011), Assimilation of upwelled nitrate by small eukaryotes in the Sargasso Sea, *Nat. Geosci.*, *4*(10), 717–722.
- Fawcett, S. E., M. W. Lomas, B. B. Ward, and D. M. Sigman (2014), The counterintuitive effect of summer-to-fall mixed layer deepening on eukaryotic new production in the Sargasso Sea, *Global Biogeochem. Cycles*, *28*, 86–102, doi:10.1002/2013GB004579.
- Freyer, H. D. (1978), Seasonal trends of NH_4^+ and NO_3^- nitrogen isotope composition in rain collected at Jülich, Germany, *Tellus*, *30*(1), 83–92.
- Galloway, J. N., G. E. Likens, W. C. Keene, and J. M. Miller (1982), The composition of precipitation in remote areas of the world, *J. Geophys. Res.*, *87*(NC11), 8771–8786, doi:10.1029/JC087iC11p08771.
- Galloway, J. N., W. C. Keene, R. S. Artz, J. M. Miller, T. M. Church, and A. H. Knap (1989), Processes controlling the concentrations of SO_4^{2-} , NO_3^- , NH_4^+ , H^+ , HCO_3^- and CH_3COO^- in precipitation on Bermuda, *Tellus B*, *41B*(4), 427–443.
- Galloway, J. N., W. C. Keene, and G. E. Likens (1996), Processes controlling the composition of precipitation at a remote southern hemispheric location: Torres del Paine National Park, Chile, *J. Geophys. Res.*, *101*(D3), 6883–6897, doi:10.1029/95JD03229.
- Galloway, J. N., J. D. Aber, J. W. Erisman, S. P. Seitzinger, R. W. Howarth, E. B. Cowling, and B. J. Cosby (2003), The nitrogen cascade, *BioScience*, *53*(4), 341–356.
- Galloway, J. N., et al. (2004), Nitrogen cycles: Past, present, and future, *Biogeochemistry*, *70*(2), 153–226.
- Galloway, J. N., A. R. Townsend, J. W. Erisman, M. Bekunda, Z. Cai, J. R. Freney, L. A. Martinelli, S. P. Seitzinger, and M. A. Sutton (2008), Transformation of the nitrogen cycle: Recent trends, questions, and potential solutions, *Science*, *320*(5878), 889–892.
- Hastings, M. G., D. M. Sigman, and F. Lipschultz (2003), Isotopic evidence for source changes of nitrate in rain at Bermuda, *J. Geophys. Res.*, *108*(D24), 4790, doi:10.1029/2003JD003789.
- Hastings, M. G., J. C. Jarvis, and E. J. Steig (2009), Anthropogenic impacts on nitrogen isotopes of ice-core nitrate, *Science*, *324*(5932), 1288, doi:10.1126/science.1170510.
- Heaton, T. H. E. (1987), $^{15}\text{N}/^{14}\text{N}$ ratios of nitrate and ammonium in rain at Pretoria, South Africa, *Atmos. Environ.* (1967), *21*(4), 843–852.
- Heaton, T. H. E., B. Spiro, and S. M. C. Robertson (1997), Potential canopy influences on the isotopic composition of nitrogen and sulphur in atmospheric deposition, *Oecologia*, *109*(4), 600–607.
- Hermes, J. D., P. M. Weiss, and W. W. Cleland (1985), Use of nitrogen-15 and deuterium isotope effects to determine the chemical mechanism of phenylalanine ammonia-lyase, *Biochemistry*, *24*(12), 2959–2967.
- Holmes, R. M., J. W. McClelland, D. M. Sigman, B. Fry, and B. J. Peterson (1998), Measuring $^{15}\text{N}-\text{NH}_4^+$ in marine, estuarine and fresh waters: An adaptation of the ammonia diffusion method for samples with low ammonium concentrations, *Mar. Chem.*, *60*(3–4), 235–243.
- Jia, G., and F. Chen (2010), Monthly variations in nitrogen isotopes of ammonium and nitrate in wet deposition at Guangzhou, south China, *Atmos. Environ.*, *44*(19), 2309–2315.
- Jickells, T. D., S. D. Kelly, A. R. Baker, K. Biswas, P. F. Dennis, L. J. Spokes, M. Witt, and S. G. Yeatman (2003), Isotopic evidence for a marine ammonia source, *Geophys. Res. Lett.*, *30*(7), 1374, doi:10.1029/2002GL016728.
- Johnson, M. T. (2010), A numerical scheme to calculate temperature and salinity dependent air-water transfer velocities for any gas, *Ocean Sci.*, *6*(4), 913–932.
- Johnson, M. T., and T. G. Bell (2008), Coupling between dimethylsulfide emissions and the ocean-atmosphere exchange of ammonia, *Environ. Chem.*, *5*(4), 259–267.
- Johnson, M. T., P. S. Liss, T. G. Bell, T. J. Lesworth, A. R. Baker, A. J. Hind, T. D. Jickells, K. F. Biswas, E. M. S. Woodward, and S. W. Gibb (2008), Field observations of the ocean-atmosphere exchange of ammonia: Fundamental importance of temperature as revealed by a comparison of high and low latitudes, *Global Biogeochem. Cycles*, *22*, GB1019, doi:10.1029/2007GB003039.
- Jung, J., H. Furutani, and M. Uematsu (2011), Atmospheric inorganic nitrogen in marine aerosol and precipitation and its deposition to the North and South Pacific Oceans, *J. Atmos. Chem.*, *68*(2), 157–181.
- Kasper-Giebl, A., M. F. Kalina, and H. Puxbaum (1999), Scavenging ratios for sulfate, ammonium and nitrate determined at Mt. Sonnblick (3106 m a.s.l.), *Atmos. Environ.*, *33*(6), 895–906.
- Kawashima, H., and T. Kurahashi (2011), Inorganic ion and nitrogen isotopic compositions of atmospheric aerosols at Yurihonjo, Japan: Implications for nitrogen sources, *Atmos. Environ.*, *45*(35), 6309–6316.
- Keene, W. C., A. A. P. Pszenny, J. N. Galloway, and M. E. Hawley (1986), Sea-salt corrections and interpretation of constituent ratios in marine precipitation, *J. Geophys. Res.*, *91*(D6), 6647–6658, doi:10.1029/JD091iD06p06647.
- Keene, W. C., J. L. Moody, J. N. Galoway, J. M. Prospero, O. R. Cooper, S. Eckhardt, and J. R. Maben (2014), Long-term trends in aerosol and precipitation composition over the western North Atlantic Ocean at Bermuda, *Atmos. Chem. Phys.*, *14*, 8119–8135, doi:10.5194/acp-14-8119-2014.
- Kirshenbaum, I., J. S. Smith, T. Crowell, J. Graff, and R. McKee (1947), Separation of the nitrogen isotopes by the exchange reaction between ammonia and solutions of ammonium nitrate, *J. Chem. Phys.*, *15*(7), 440–446.
- Knapp, A. N., M. G. Hastings, D. M. Sigman, F. Lipschultz, and J. N. Galloway (2010), The flux and isotopic composition of reduced and total nitrogen in Bermuda rain, *Mar. Chem.*, *120*(1–4), 83–89.

- Knapp, A. N., D. M. Sigman, F. Lipschultz, A. B. Kustka, and D. G. Capone (2011), Interbasin isotopic correspondence between upper-ocean bulk DON and subsurface nitrate and its implications for marine nitrogen cycling, *Global Biogeochem. Cycles*, *25*, GB4004, doi:10.1029/2010GB003878.
- Lipschultz, F. (2001), A time-series assessment of the nitrogen cycle at BATS, *Deep Sea Res., Part II*, *48*(8–9), 1897–1924.
- Liss, P. S., and P. G. Slater (1974), Flux of gases across the air-sea interface, *Nature*, *247*(5438), 181–184.
- Lomas, M. W., N. R. Bates, R. J. Johnson, A. H. Knap, D. K. Steinberg, and C. A. Carlson (2013), Two decades and counting: 24-years of sustained open ocean biogeochemical measurements in the Sargasso Sea, *Deep Sea Res., Part II*, *93*, 16–32, doi:10.1016/j.dsr2.2013.01.008.
- Macko, S. A., M. L. F. Estep, M. H. Engel, and P. E. Hare (1986), Kinetic fractionation of stable nitrogen isotopes during amino acid transamination, *Geochim. Cosmochim. Acta*, *50*(10), 2143–2146.
- McIlvin, M. R., and M. A. Altabet (2005), Chemical conversion of nitrate and nitrite to nitrous oxide for nitrogen and oxygen isotopic analysis in freshwater and seawater, *Anal. Chem.*, *77*(17), 5589–5595.
- Mészáros, E., and T. Szentimrei (1985), On the wet removal of gaseous and particulate sulfur and nitrogen species from the atmosphere, *J. Atmos. Chem.*, *2*(4), 405–413.
- Moody, J. L., and J. N. Galloway (1988), Quantifying the relationship between the atmospheric transport and the chemical composition of precipitation on Bermuda, *Tellus B*, *40B*, 463–479, doi:10.1111/j.1600-0889.1988.tb00117.x.
- Moore, H. (1977), The isotopic composition of ammonia, nitrogen dioxide and nitrate in the atmosphere, *Atmos. Environ.* (1967), *11*(12), 1239–1243.
- Morin, S., J. Savarino, M. M. Frey, F. Domine, H. W. Jacobi, L. Kaleschke, and J. M. F. Martins (2009), Comprehensive isotopic composition of atmospheric nitrate in the Atlantic Ocean boundary layer from 65°S to 79°N, *J. Geophys. Res.*, *114*, D05303, doi:10.1029/2008JD010696.
- National Atmospheric Deposition Program (2007), *National Atmospheric Deposition Program (NRSP-3)*, edited by N. P. Office, Ill. State Water Surv., Champaign.
- Norman, M., and C. Leck (2005), Distribution of marine boundary layer ammonia over the Atlantic and Indian Oceans during the Aerosols99 cruise, *J. Geophys. Res.*, *110*, D16302, doi:10.1029/2005JD005866.
- Paerl, H. W., R. L. Dennis, and D. R. Whittall (2002), Atmospheric deposition of nitrogen: Implications for nutrient over-enrichment of coastal waters, *Estuaries*, *25*(4B), 677–693.
- Pavuluri, C. M., K. Kawamura, E. Tachibana, and T. Swaminathan (2010), Elevated nitrogen isotope ratios of tropical Indian aerosols from Chennai: Implication for the origins of aerosol nitrogen in South and Southeast Asia, *Atmos. Environ.*, *44*(29), 3597–3604.
- Pinder, R. W., P. J. Adams, S. N. Pandis, and A. G. Gilliland (2006), Temporally resolved ammonia emission inventories: Current estimates, evaluation tools, and measurement needs, *J. Geophys. Res.*, *111*, D16310, doi:10.1029/2005JD006603.
- Quinn, P. K., R. J. Charlson, and W. H. Zoller (1987), Ammonia, the dominant base in the remote marine troposphere: A review, *Tellus B*, *39B*(5), 413–425.
- Quinn, P. K., R. J. Charlson, and T. S. Bates (1988), Simultaneous observations of ammonia in the atmosphere and ocean, *Nature*, *335*, 120–121.
- Quinn, P. K., W. E. Asher, and R. J. Charlson (1992), Equilibria of the marine multiphase ammonia system, *J. Atmos. Chem.*, *14*(1), 11–30.
- Quinn, P. K., K. J. Barrett, F. J. Dentener, F. Lipschultz, and K. D. Six (1996), Estimation of the air sea exchange of ammonia for the North Atlantic Basin, *Biogeochemistry*, *35*(1), 275–304.
- Russell, K. M., J. N. Galloway, S. A. Macko, J. L. Moody, and J. R. Scudlark (1998), Sources of nitrogen in wet deposition to the Chesapeake Bay region, *Atmos. Environ.*, *32*(14–15), 2453–2465.
- Shimshock, J. P., and R. G. De Pena (1989), Below-cloud scavenging of tropospheric ammonia, *Tellus B*, *41B*(3), 296–304.
- Sigman, D. M., K. L. Casciotti, M. Andreani, C. Barford, M. Galanter, and J. K. Bohlke (2001), A bacterial method for the nitrogen isotopic analysis of nitrate in seawater and freshwater, *Anal. Chem.*, *73*(17), 4145–4153.
- Silfer, J. A., M. H. Engel, and S. A. Macko (1992), Kinetic fractionation of stable carbon and nitrogen isotopes during peptide bond hydrolysis: Experimental evidence and geochemical implications, *Chem. Geol. Isot. Geosci. Sect.*, *101*(3–4), 211–221.
- Thode, H. G., R. L. Graham, and J. A. Ziegler (1945), A mass spectrometer and the measurement of isotope exchange factors, *Can. J. Res.*, *23b*(1), 40–47.
- Urey, H. C. (1947), The thermodynamic properties of isotopic substances, *J. Chem. Soc.*, *1947*, 562–581, doi:10.1039/JR9470000562.
- Wankel, S. D., Y. Chen, C. Kendall, A. F. Post, and A. Paytan (2010), Sources of aerosol nitrate to the Gulf of Aqaba: Evidence from $\delta^{15}\text{N}$ and $\delta^{18}\text{O}$ of nitrate and trace metal chemistry, *Mar. Chem.*, *120*(1–4), 90–99.
- Xu, L., and J. E. Penner (2012), Global simulations of nitrate and ammonium aerosols and their radiative effects, *Atmos. Chem. Phys.*, *12*(20), 9479–9504.
- Yeatman, S. G., L. J. Spokes, P. F. Dennis, and T. D. Jickells (2001), Comparisons of aerosol nitrogen isotopic composition at two polluted coastal sites, *Atmos. Environ.*, *35*(7), 1307–1320.
- Zhang, L., M. A. Altabet, T. Wu, and O. Hadas (2007), Sensitive measurement of NH_4^+ $^{15}\text{N}/^{14}\text{N}$ ($\delta^{15}\text{N}_{\text{NH}_4^+}$) at natural abundance levels in fresh and saltwaters, *Anal. Chem.*, *79*(14), 5297–5303.
- Zhang, Y., X. J. Liu, A. Fangmeier, K. T. W. Goulding, and F. S. Zhang (2008), Nitrogen inputs and isotopes in precipitation in the North China Plain, *Atmos. Environ.*, *42*(7), 1436–1448.